Simultaneous photoacoustic and optical attenuation imaging of single cells using photoacoustic microscopy

Michael J. Moore, Eric M. Strohm, and Michael C. Kolios

[1]Department of Physics, Ryerson University, Toronto, Canada
[2]Institute for Biomedical Engineering, Science and Technology (iBEST), a partnership between Ryerson University and St. Michael's Hospital, Toronto, Canada
[3]Keenan Research Centre for Biomedical Science of St. Michael's Hospital, Toronto, Canada

ABSTRACT

A new technique for simultaneously acquiring photoacoustic images as well as images based on the optical attenuation of single cells in a human blood smear was developed. An ultra-high frequency photoacoustic microscope equipped with a 1 GHz transducer and a pulsed 532 nm laser was used to generate the images. The transducer and 20X optical objective used for laser focusing were aligned coaxially on opposing sides of the sample. Absorption of laser photons by the sample yielded conventional photoacoustic (PA) signals, while incident photons which were not attenuated by the sample were absorbed by the transducer, resulting in the formation of a photoacoustic signal (tPA) within the transducer itself. Both PA and tPA signals, which are separated in time, were recorded by the system in a single RF-line. Areas of strong signal in the PA images corresponded to dark regions in the tPA images. Additional details, including the clear delineation of the cell cytoplasm and features in red blood cells, were visible in the tPA image but not the corresponding PA image. This imaging method has applications in probing the optical absorption and attenuation characteristics of biological cells with sub-cellular resolution.

Keywords: Photoacoustic Microscopy, optical attenuation, imaging

1. INTRODUCTION

Photoacoustic microscopy (PAM) is an emerging technique with widespread application in the fields of biology and medicine. The versatility of PAM is demonstrated by the numerous studies conducted with the technology, ranging from super resolution imaging,[1] to quantitative and functional analysis of single biological cells.[2,3] PAM has been used to produce diffraction limited images reflecting the spatial distribution of endogenous cellular chromophores including: hemoglobin, melanin, cytochrome, and DNA.[4] The amplitude of the photoacoustic (PA) signals in these images is directly proportional to the optical absorption coefficient of the target chromophore.[5] For this reason the PAM technique has previously been used for quantitative assessment of the optical absorption properties of various solids and inks;[6–8] however, as it can only assess optical absorption, PAM affords incomplete information about the optical attenuation properties of the sample. In this work, we present a new method that uses an ultra-high frequency photoacoustic microscope (UHF-PAM) to acquire simultaneous conventional PA images and images based on the optical attenuation of the sample.

The ultra-high frequency (UHF) ultrasonic transducers used in acoustic microscopy have central frequencies and bandwidths in the hundreds of megahertz (MHz). An UHF transducer typically consists of a piezoelectric layer of zinc oxide epitaxially grown between two gold electrodes on top of a sapphire buffer rod.[9–11] In pulse-echo measurements, plane waves generated by the piezoelectric element propagate through the buffer rod and are focused to convergent spherical waves by a hemispherical aperture ground into the bottom of the rod.[11,12] After interaction with the sample, the reflected ultrasound waves travel through the buffer rod and are converted to electrical signals by the piezoelectric element. A schematic of a complete transducer, including the piezoelectric element and buffer rod, is shown in Figure 1.
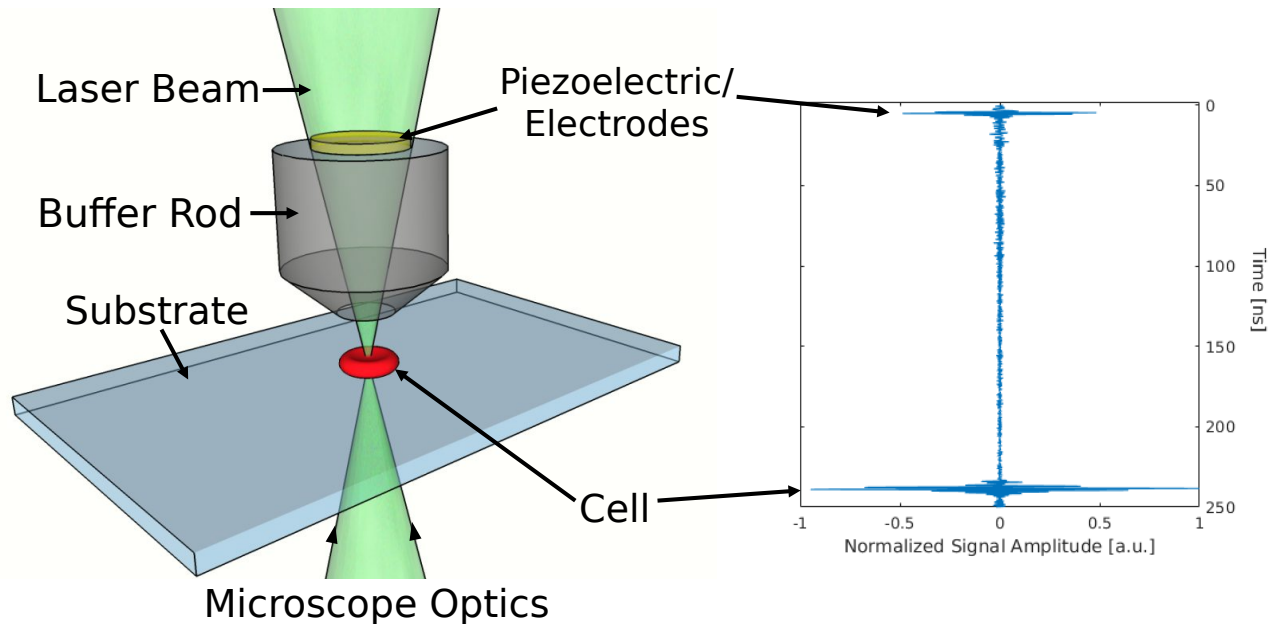
Figure 1. Left: A schematic of the UHF photoacoustic microscope setup. The laser beam focused by the microscope optics passes through the target cell and is incident on the transducer piezoelectric element. A photoacoustic signal is produced simultaneously within the transducer and the targeted cell. Right: A measured RF-line containing PA signals from both the transducer and cell. The tPA signal is recorded sooner in time than the signal from the cell, as the PA wave from the sample has a longer time of flight for reaching the transducer.

In transmission mode PAM, the microscope optics used to focus the incident laser are opposite the transducer (Fig 1). The PA waves emitted by the sample after pulsed laser excitation follow the same path as reflected ultrasound waves, propagating from the transducer focal zone into the sapphire lens before being detected by the piezoelectric element. Photons that are not absorbed or scattered away from the transducer by the sample fall incident directly upon the sapphire buffer rod. Due to the high optical transmission of sapphire in the visible spectrum,[13] these photons will subsequently hit the piezoelectric/electrode element. Since the epitaxially grown zinc oxide in the transducer has negligible absorption in the visible spectrum,[14] it is our assumption that the electrodes (or other structures within the transducer) absorb the photons and generate a PA wave internally within the transducer. We have termed PA waves generated in this manner tPA signals. These tPA signals are recorded in the same RF-line as the PA signal emitted by the sample, and are dependent upon both the optical absorption and scattering of photons by the sample.

2. METHODS

2.1 Sample Preparation

A blood smear was made from a drop of whole human blood extracted via fingerprick from a healthy volunteer in accordance with the Ryerson University Ethics Review Board (REB #2012-210) protocols. The smear was air dried and subsequently fixed by flooding the slide with ice cold methanol and allowing it to completely evaporate. One mL of Wright-Giemsa stain (Sigma Aldrich, USA) was added to the fixed slides, followed by two mL of deionized water after a period of one minute. The stain solution was left to stand at room temperature for 2 minutes before being thoroughly rinsed with deionized water and air dried.

2.2 System Setup

A modified scanning acoustic microscope (Kibero GmbH, Germany) equipped with a fiber coupled pulsed 532 nm laser (Teem Photonics, France) was used to image individual cells in the blood smear. The microscope was
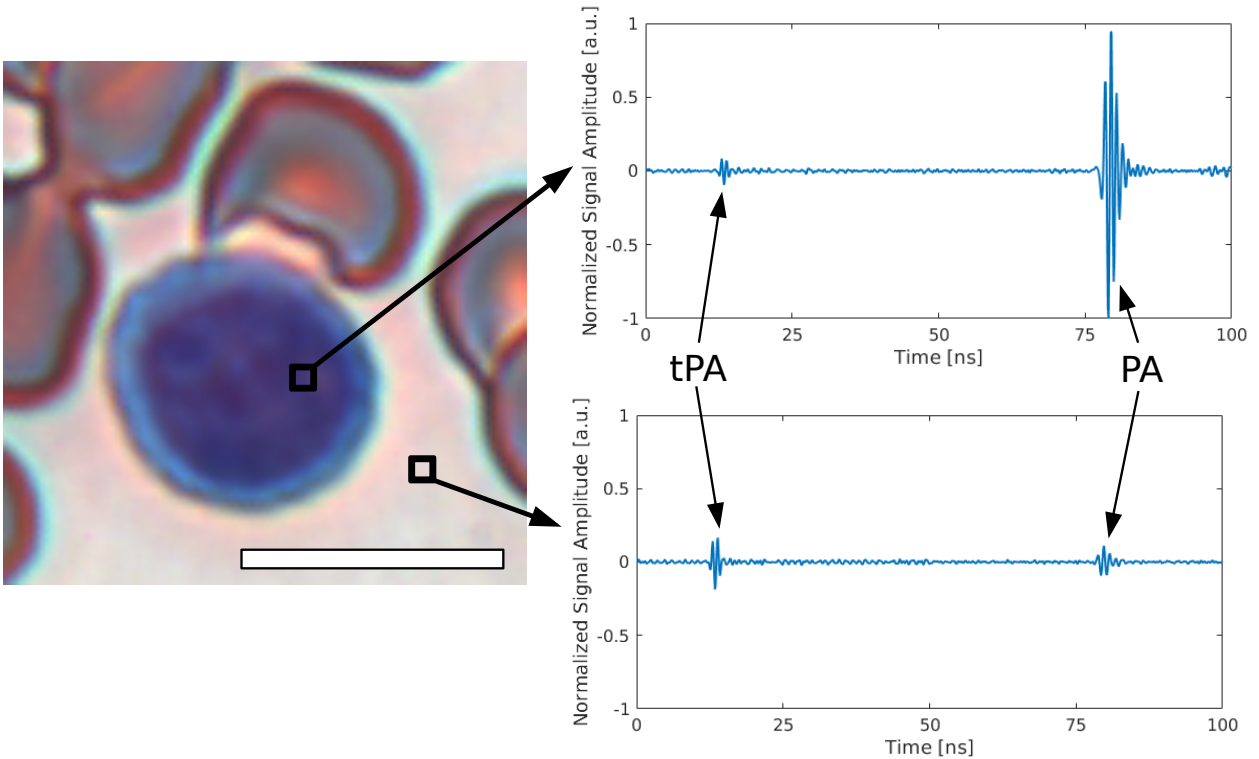
Figure 2. Left: Optical image of a human lymphocyte and red blood cells stained with Wright-Giemsa. Photoacoustic RF lines acquired from the indicated regions are shown on the right. The scale bar is 10 μm. Right: In regions with strong optical absorption (e.g. the lymphocyte nucleus), the PA signal from the sample is greater in amplitude than the tPA signal generated within the transducer. In sample regions with low optical absorption the trend is reversed. Both signals were normalized to the maximum signal amplitude in the top figure.

outfitted with an ultrasound transducer with a central frequency of 1 GHz, and the 532 nm laser had a pulse repetition frequency of 4 kHz and pulse width of 330 ps. The laser beam was directed into the microscope optical path via an optical fiber, focused through a 20X optical objective (Olympus, Japan) and was aligned confocally with the ultrasound transducer on the opposing side of the microscope translation stage. The blood smear was placed on the translation stage and a drop of deionized water was used to provide acoustic coupling between the sample and transducer. The entire system was housed in a temperature controlled enclosure maintained at 37°C for the duration of the experiment.

2.3 Image Acquisition

Target cells were visually identified using the microscope optics and were moved into the laser-transducer confocal spot via the microscope translation stage. After laser irradiation, the resultant PA signals were amplified using a 40 dB amplifier (Miteq, USA) and digitized using a 10 bit digitizer (Agilent, USA) with a sampling frequency of 8 gigasamples per second. All acquired signals were averaged 100 times to increase SNR. As illustrated in Figures 1 and 2, both the tPA signal and the signal from the target cell were captured in the acquired RF-lines. The cells were scanned in a raster pattern with a step size of 0.33 μm. After scanning, the acquired RF lines were time gated to contain only the tPA signal or the PA signal from the sample. Two Maximum Amplitude Projection (MAP) images were produced from these time gated regions by assigning each scan position a gray scale value with intensity proportional to the maximum amplitude of the RF-line acquired at that coordinate.

3. RESULTS AND DISCUSSION

3.1 Air-coupled measurements

To verify that the tPA signals were produced within the transducer, raster scans were performed without the use of any coupling medium. In this case, no photoacoustic waves generated at the sample will propagate to the buffer rod due to a combination of the high attenuation coefficient and low acoustic impedance of air,[11] and only photons which hit the transducer directly will contribute to the tPA signal. A tPA image of stained red blood cells scanned using this setup is shown on the right hand side of Figure 3. The red blood cells in the tPA image exhibit two dark rings: one around the cell perimeter, and the other in the center of the cell. Both the perimeter and concave center of the red blood cell have high curvature, and so a possible explanation for these dark regions is scattering of the tightly focused laser beam away from the transducer element due to the curved red blood cell surface and the difference in the refractive index of the red blood cell and air.

3.2 Stained Cells

Representative RF-lines from a Wright-Giemsa stained blood smear are shown in Figure 2. When a strongly stained area (e.g. the cell nucleus) was measured, the PA signal from the sample was approximately 10 fold larger than that of the tPA signal. Conversely, in areas with scant stain uptake or with residual dye persisting on the glass substrate after the rinsing process, the tPA signal was stronger. Optical images of a stained lymphocyte and a stained neutrophil are shown in Figures 4A and 4D, respectively. Deep purple/blue staining is observed in the nuclei, while light blue and light pink hues are present in the cell cytoplasm of the lymphocyte and neutrophil, respectively. The PA images from the segment of the RF-line time gated to contain only the PA signal from the sample are shown in Figures 4B and 4E. Strong PA signals were observed from the nuclei, with weaker amplitude signals from the surrounding red blood cells. In the scan of the lymphocyte, there was considerable PA signal from the cell cytoplasm; however, in the neutrophil the PA signal from the cytoplasm was low. Additional details about the trends observed in the PA images are discussed elsewhere.[15] The images shown in Figures 4C and 4F were created with the tPA time gated data. Dark regions in both tPA MAP images corresponded to regions of strong optical attenuation. Since the tPA images are based on optical scattering and absorption, this technique shows additional detail that is not observed in the PA images alone. For example, in figure 4F, the boundary of the neutrophil cytoplasm is clearly delineated, while it is difficult to see in the PA image. Additionally, the boundary of the red blood cells in 4C and 4F can clearly be seen.
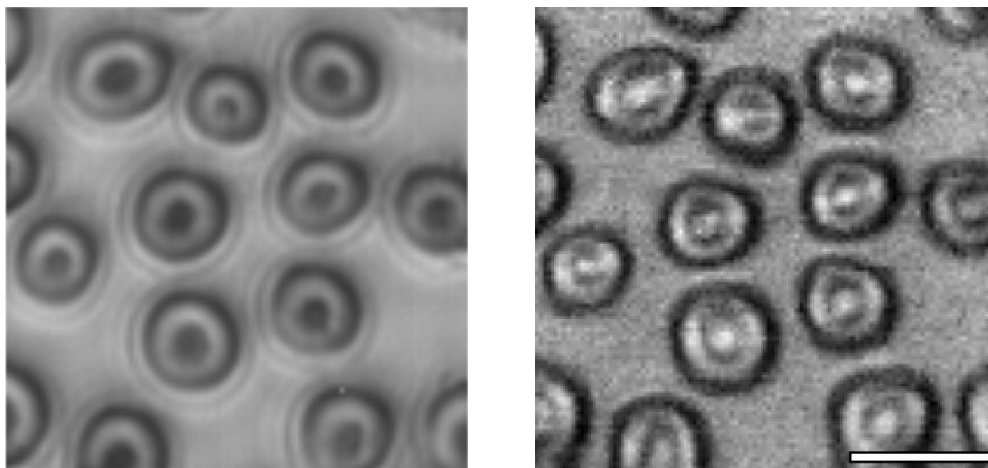

Figure 3. Left: Optical image of Wright-Giemsa stained red blood cells in a human blood smear. Right: Corresponding tPA image acquired using an air coupling medium. Dark rings are observed around the perimeter and center of the red blood cells. The scale bar is 10 μm.
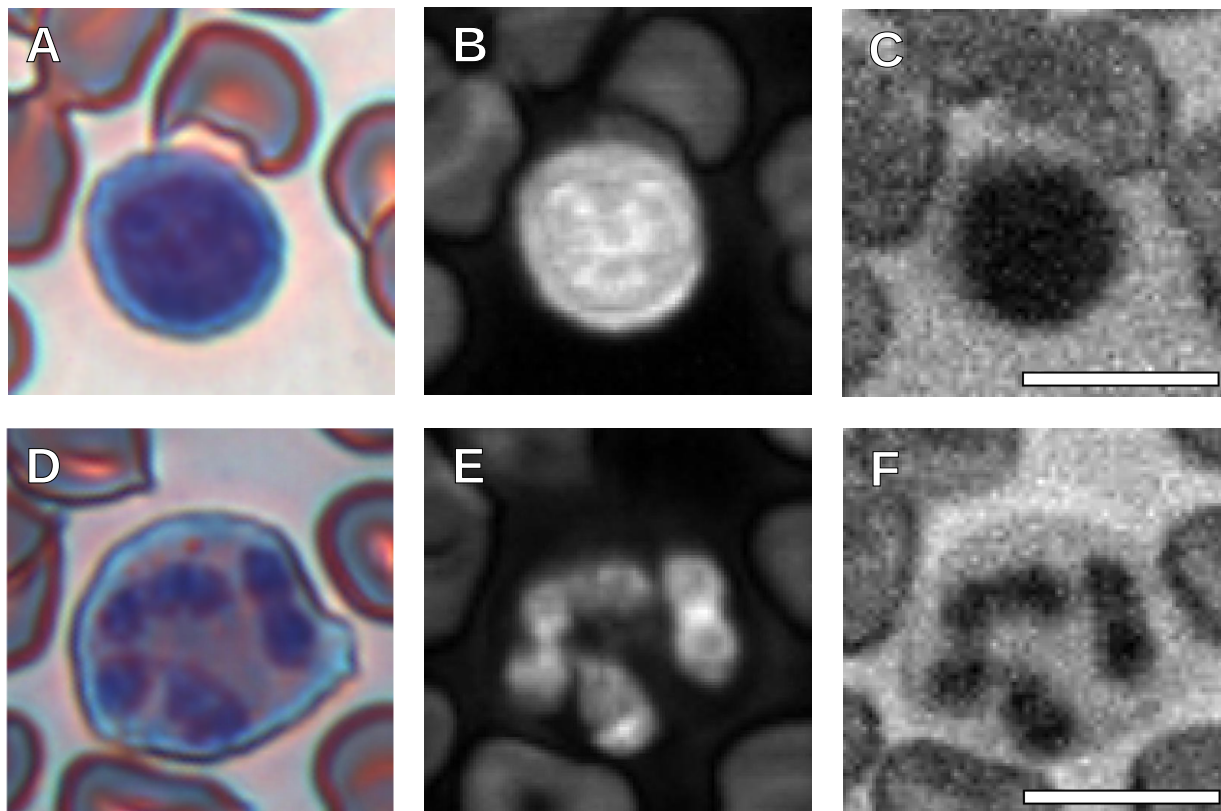
Figure 4. A) Optical image of a human lymphocyte and red blood cells stained with Wright Giemsa. B) Image generated with the PA signal gated RF-lines. C) Corresponding tPA image based on optical attenuation through the cell. D) Optical image of an human neutrophil and red blood cells. E) PA image of the stained neutrophil and surrounding red blood cells. F) Corresponding neutrophil tPA image. The contour of the cell cytoplasm and surrounding red blood cells can clearly be seen. The scale bars are 10 μm.

Figures 3 and 4 demonstrate that the tPA images exhibit unique features that are not visible in conventional PA images. The accentuation of features in the tPA images, especially in areas of high curvature, may be useful when trying to delineate weakly absorbing cells which produce negligible PA signal. Additionally, because the tPA signals can be acquired without the use of an acoustic coupling medium, this technique may be useful for examining samples which cannot be submerged in water.

4. CONCLUSION

A new technique for simultaneously acquiring images based on both the PA signals and optical attenuation of individual biological cells was developed. Images of stained leukocytes and red blood cells were acquired, and in all cases the image resulting from the tPA signal was shown to contain features not present in the PA image from the sample. In the future, refinement of this technique may allow for quantification and extraction of optical attenuation properties from the tPA images, and examination of samples that cannot be submerged in water.

ACKNOWLEDGMENTS

REFERENCES

[1] Danielli, A., Maslov, K., Garcia-Uribe, A., Winkler, A. M., Li, C., Wang, L., Chen, Y., Dorn, G. W., and Wang, L. V., "Label-free photoacoustic nanoscopy," *Journal of Biomedical Optics* **19**(8), 086006 (2014).

[2] Strohm, E. M. and Kolios, M. C., "Classification of Blood Cells and Tumor Cells Using Label-Free Ultrasound and Photoacoustics," *Cytometry Part A* **87**, 741–749 (2015).

[3] Wang, L., Maslov, K., and Wang, L. V., "Single-cell label-free photoacoustic flowoxigraphy in vivo," *Proceedings of the National Academy of Sciences of the United States of America* **110**(15), 5759–64 (2013).

[4] Strohm, E. M., Moore, M. J., and Kolios, M. C., "Single cell photoacoustic microscopy: a review," *IEEE Journal of Selected Topics in Quantum Electronics* **22**(3), 6801215 (2015).

[5] Yao, J. and Wang, L. V., "Sensitivity of photoacoustic microscopy," *Photoacoustics* **2**, 87–101 (2014).

[6] Hordvik, A. and Schlossberg, H., "Photoacoustic technique for determining optical absorption coefficients in solids," *Applied Optics* **16**(1), 101–7 (1977).

[7] Yuan, Z. and Jiang, H., "Quantitative photoacoustic tomography: Recovery of optical absorption coefficient maps of heterogeneous media," *Applied Physics Letters* **88**(231101), 1–3 (2006).

[8] Li, Z., Li, H., Zeng, Z., Xie, W., and Chen, W. R., "Determination of optical absorption coefficient with focusing photoacoustic imaging," *Journal of Biomedical Optics* **17**(6), 0612161–6 (2012).

[9] Reeder, T. M. and Winslow, D. K., "Characteristics of Microwave Acoustic Transducers for Volume Wave Excitation," *IEEE Transactions on Microwave Theory and Techniques* **MTT-17**(11), 927–941 (1969).

[10] Chou, C.-H., Khuri-Yakub, B. T., and Kino, G. S., "Lens design for acoustic microscopy," *IEEE Transactions on Ultrasonics, Ferroelectrics, and Frequency Control* **35**(4), 464–469 (1988).

[11] Briggs, Andrew and Kolosov, Oleg, [*Acoustic Microscopy, 2ed.*], Oxford University Press (2009).

[12] Quate, C. F., Atalar, A., and Wickramasinghe, H. K., "Acoustic microscopy with mechanical scanning. A review," *Proceedings of the IEEE* **67**(8), 1092–1114 (1979).

[13] Dobrovinskaya, Elena R. and Lytvynov, Leonid A. and Pishchik, Valerian, [*Sapphire: Material, Manufacturing, Applications*], Springer (2009).

[14] Sun, X. W. and Kwok, H. S., "Optical properties of epitaxially grown zinc oxide films on sapphire by pulsed laser deposition," *Journal of Applied Physics* **86**(1), 408–411 (1999).

[15] Strohm, E. M., Moore, M. J., and Kolios, M. C., "High resolution ultrasound and photoacoustic imaging of single cells," *Photoacoustics* **In Press** (2016).